Clay Minerals (1999) **34**, 99–108

Effects of acid mine drainage on clay minerals suspended in the Tinto River (Río Tinto, Spain). An experimental approach

E. GALAN, M. I. CARRETERO AND J. C. FERNANDEZ-CALIANI*

*Dpto. de Cristalografía y Mineralogía, Facultad de Química, Universidad de Sevilla, Spain, and *Dpto. de Geología, Facultad de Ciencias Experimentales, Universidad de Huelva, Spain*

(*Received 3 September 1997; revised 2 September 1998*)

ABSTRACT: The Tinto river is one of the most polluted stream environments in the world, as a result of both acid mine drainage and natural acid rock drainage. Two representative samples from the phyllosilicate-rich rocks exposed in the drainage basin (Palaeozoic chlorite-bearing slates and Miocene smectite-rich marls) were treated with acid river water (pH = 2.2) for different times to constrain the effects of extreme hydrogeochemical conditions on clay mineral stability. Illite and kaolinite did not show appreciable variations in their crystal chemistry parameters upon treatment. Chlorite underwent an incipient chemical degradation evidenced by the progressive loss of Fe in octahedral positions coupled with a shortening of the *b* unit-cell parameter, although no weathering products of chlorite were observed. Smectite and calcite were rapidly and fully dissolved thus neutralizing the water acidity, and subsequently Fe and Al oxy-hydroxides and opaline silica precipitated from the aqueous solution, together with a neoformed amorphous silicate phase largely enriched in Al and Mg.

The Tinto river is one of the most polluted fluvial environments in the world because of natural processes and particularly as a consequence of the large-scale mining on its mineralized catchment since prehistoric times. The river's source is near the Río Tinto mines and close to here it receives the water emanating from both surface and underground mine workings, wastes and sulphide-rich tailings. As a result of acid-mine drainage, the river water shows a typical wine-red colour and it is characterized by very acidic pH values (2–4 for most of its length) and high concentrations of heavy metals (especially Fe, Cu and Zn) and sulphates (Nelson & Lamothe, 1993; Elbaz-Poulichet & Leblanc, 1996). Suspended and ochreous overbank sediments are also severely contaminated by heavy metals throughout the river course (Cabrera *et al*., 1992; Fernández-Caliani *et al*., 1996).

The river drains different geological formations consisting, in its upstream area, of Devonian-Carboniferous slates, quartzites and volcano-sedimentary rocks. Associated with the latter are interbedded, large polymetallic massive sulphides of the Río Tinto mining district (Schermerhörn, 1971; García-Palomero, 1980). In its lower course, the Tinto flows through Cenozoic sedimentary formations made up predominantly of clays and marls belonging to the Guadalquivir basin (Galán & González, 1993). Finally, the river discharges into the Atlantic ocean after its confluence with the Odiel river, another acid fluvial system, forming the Huelva estuary on the Southwestern Spanish coast (Fig. 1).

As we have reported in previous papers (Fernández-Caliani *et al*., 1996; Galán *et al*., 1996), the mineral composition of the particulate matter suspended in the river is largely controlled by the source-area lithology and soil types exposed regionally in the drainage basin, and so the mineral assemblages reflect, at least in part, the inherited detrital character of the suspended sediments. Thus, the suspended load is essentially composed of a complex mixture of clay minerals (illite+kaolinite ±

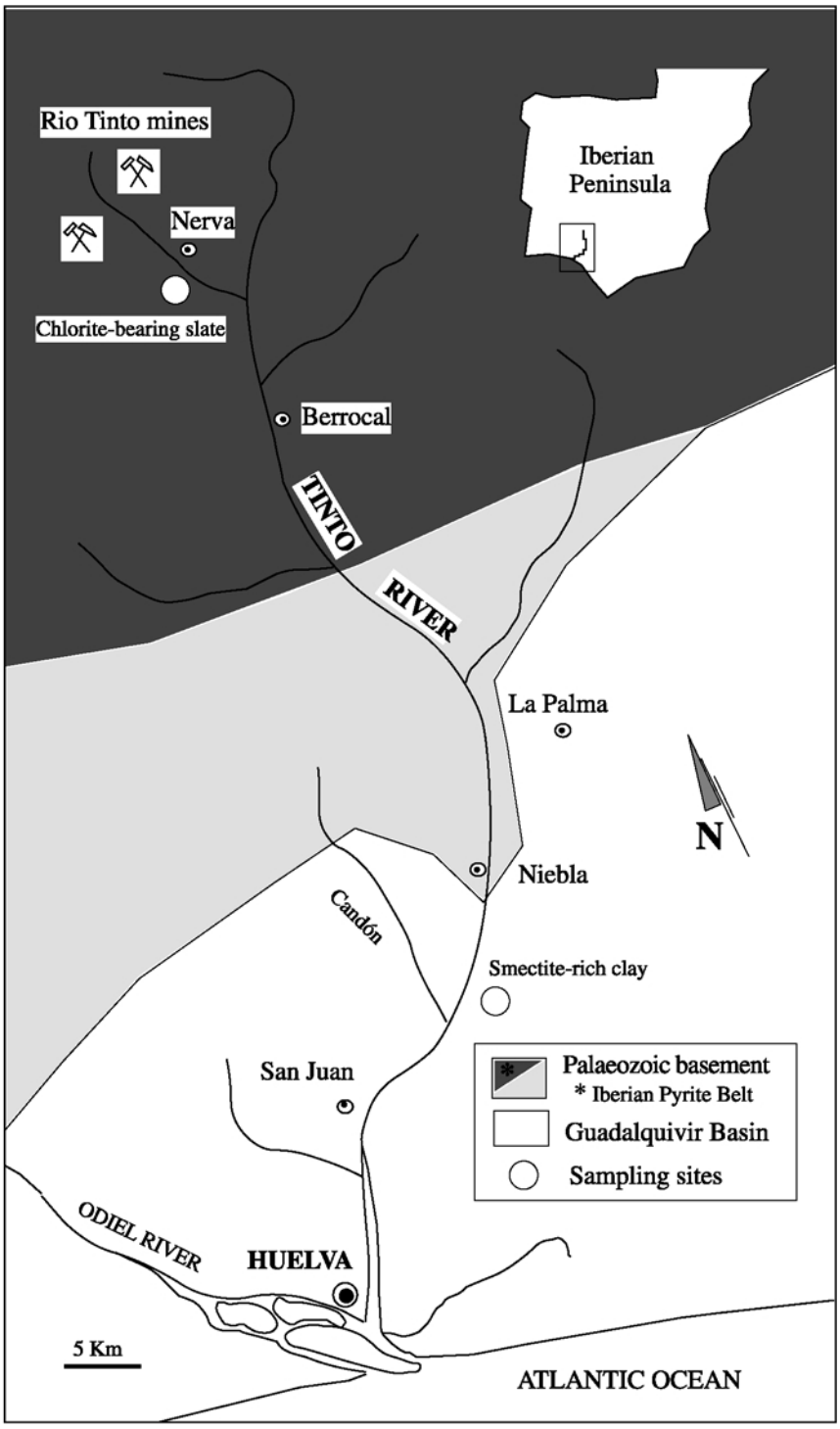

FIG. 1. Location map of the Tinto river showing sampling sites.

chlorite), poorly crystalline phases and inorganic amorphous components (iron oxides and hydroxides), with minor amounts of quartz and feldspars. A relevant observation was the general lack of smectites in suspended sediments, in spite of the fact that they are well represented in both the clayey sediments drained by the water flow and the inputs of unpolluted clays from tributaries.

This work is an attempt to constrain the effects of acid sulphate water on clay mineral stability with a laboratory simulation of the extreme hydrogeochemical conditions in the Tinto river. The simulation is intended to monitor both the mineralogical changes in the sediments and the exchange reactions between the suspended sediment and river water, induced by acid mine drainage.

EXPERIMENTAL

Two representative samples of the phyllosilicate materials exposed in the drainage basin were selected. The first is a Palaeozoic chlorite-bearing slate collected at the head of the stream, and the second corresponds to Miocene smectite-rich clays cropping out at the stream's lower course. The location of the sampling sites is shown in Fig. 1. River water was sampled with polyethylene bottles and filtered within 24 h of its collection, whereas pH and temperature values were recorded *in situ.*

Mineral composition was determined by X-ray diffraction (XRD) on a Philips powder diffractometer equipped with an automatic slit, using Ni-filtered Cu-$K\alpha$ radiation at 20 mA, 40 kV, and a scanning speed of 1°2θ per min. Previously, the slate sample was reduced to powder by grinding, and the required particle size-fraction (<63 μm) was obtained by sieving. For clay mineral analysis, the <2 μm fractions were separated by centrifugation, and well-oriented aggregates were prepared by sedimentation of clay suspension on glass slides. Samples were pretreated with hydrogen peroxide to eliminate organic matter and with acetic acid to remove carbonates. Identification of clay minerals was carried out following the routine procedures, including the standard treatments of solvation with ethylene glycol and dimethyl sulphoxide, and heating at 550°C for 2 h. Mineral abundance was estimated by measuring the intensity of diagnostic diffraction peaks, taking into account the relative intensities proposed by Schultz (1964) and Martín Pozas (1975). Correction factors were applied for a diffractometer with an automatic slit.

The phyllosilicate crystal parameters determined on the XRD patterns were: 1) the illite and chlorite crystallinity indices, measured by the width of the peak at half-height of the basal reflection at 10 Å and 7 Å respectively, and bearing in mind Kisch's (1991) recommendations; and 2) the b_o parameter of chlorite, measured on randomly oriented powder diffractograms, based on the $d(060)$ spacing and using the quartz 211 peak as an internal standard.

For experimental simulation, six subsamples each (<63 μm) of 0.5 g dry wt of the original samples were treated at room temperature with 25 cm^3 acid sulphate water collected from the Tinto river. Acid attack was achieved using an orbital agitator permitting full contact between the solid particles and aqueous solution for different lengths of time (5, 10, 15, 30, 60 and 180 min for the clay sample; and 30, 60, 120, 180 and 360 min and 1 day for the slate sample). After treatment, the solid samples were removed by filtration, air dried, and subsequently analysed for mineralogical composition by XRD, and the aqueous solution was recovered for pH and chemical analysis.

Chemical analysis for Ca, Mg, Fe, Na and K on extracted water samples were performed by atomic absorption spectrometry (Na and K by emission) with a Perkin Elmer apparatus, whereas Si and Al were colorimetrically determined by means of an UV-visible spectrophotometer. The total dissolved sulphate concentration was determined by turbidimetry, after precipitation with barium acetate.

Additional techniques were employed, such as polarized light microscopy and scanning electron microscopy (SEM) to obtain further information concerning textural and microstructural features, as well as energy-dispersive spectroscopy (EDS) to obtain mineral chemistry data and for greater accuracy of mineral identification.

RESULTS

Starting materials

The Palaeozoic slate sample is composed essentially of phyllosilicates and quartz representing >90 wt% of the bulk sample. Significant amounts of feldspars, iron oxides, organic matter and a variety of accessory heavy minerals, such as pyrite, zircon, rutile and tourmaline, were also detected under the polarizing microscope.

Mica is the most abundant sheet silicate (Table 1). It is a well-crystallized dioctahedral 2*M*

TABLE 1. Quantitative mineral composition of the smectite-rich marl and chlorite-bearing slate samples, before and after treatment.

Miocene smectite-rich clay

Before treatment Bulk sample (%)		<63 μm (%)		<2 μm (%)	
Phyllosilicates	64	Illite	67	Illite	22
Quartz	18	Kaolinite	21	Kaolinite	8
Feldspars	<5	Smectite	12	Smectite	70
Calcite	14				
After treatment Bulk sample (%)		<63 μm (%)		<2 μm (%)	
Phyllosilicates	73	Illite	76	Illite	74
Quartz	23	Kaolinite	24	Kaolinite	26
Feldspars	<5	Smectite	0	Smectite	0
Calcite	0				

Palaeozoic chlorite-bearing slate

Before and after treatment Bulk sample (%)	
Mica	38
Chlorite	20
Quartz	35
Feldspars	<5
Heavy minerals	<5

muscovite, with a crystallinity index of ~0.25°2θ. Chlorite accounts for 20 wt% of the bulk sample. Based on its b_o parameter value (9.33 Å), chlorite has an Fe-rich composition close to chamosite, with a *IIb* polytype according to reflections shown by Moore & Reynolds (1989). In general, mica and chlorite crystals display a preferred orientation forming a well-developed slaty cleavage.

The Miocene sediment sample consists largely of very thin flakes of phyllosilicates (64 wt%) with minor percentages of quartz, calcite and feldspars. Although the <63 μm fraction contains up to 67% illite with a crystallinity index at ~0.5°2θ and 21% kaolinite showing a low degree of crystalline order, the clay fraction (<2 μm) is clearly dominated by smectite.

Reaction products

Chlorite-bearing slate. The chlorite-bearing slate remains apparently unaffected upon treatment as the relative proportions of each mineral species are virtually identical in both treated and untreated samples (Table 1). Consequently, there is no experimental evidence for either mineralogical transformation or neoformation. A comprehensive XRD study on clay minerals reveals, however, some differences in their crystallinity indices and crystal chemistry parameters (Fig. 2), reflecting an incipient degradation.

The crystallinity index of chlorite remains nearly constant during treatment; however, the b_o parameter decreases as a function of time, although the progress of shortening appears to be non-linear (Fig. 3). Moreover, EDS analysis on chlorite crystals show that the Fe/(Fe+Mg) ratio decreased from 0.85 to 0.76 for 24 h upon treatment (Fig. 4), which is fairly consistent with the shortening of the *b* unit-cell dimension inferred by XRD (e.g. Bailey, 1972, and references therein). The experimental curves given in Figs. 3 and 4 show a similar trend suggesting that the extent of the total Fe loss is

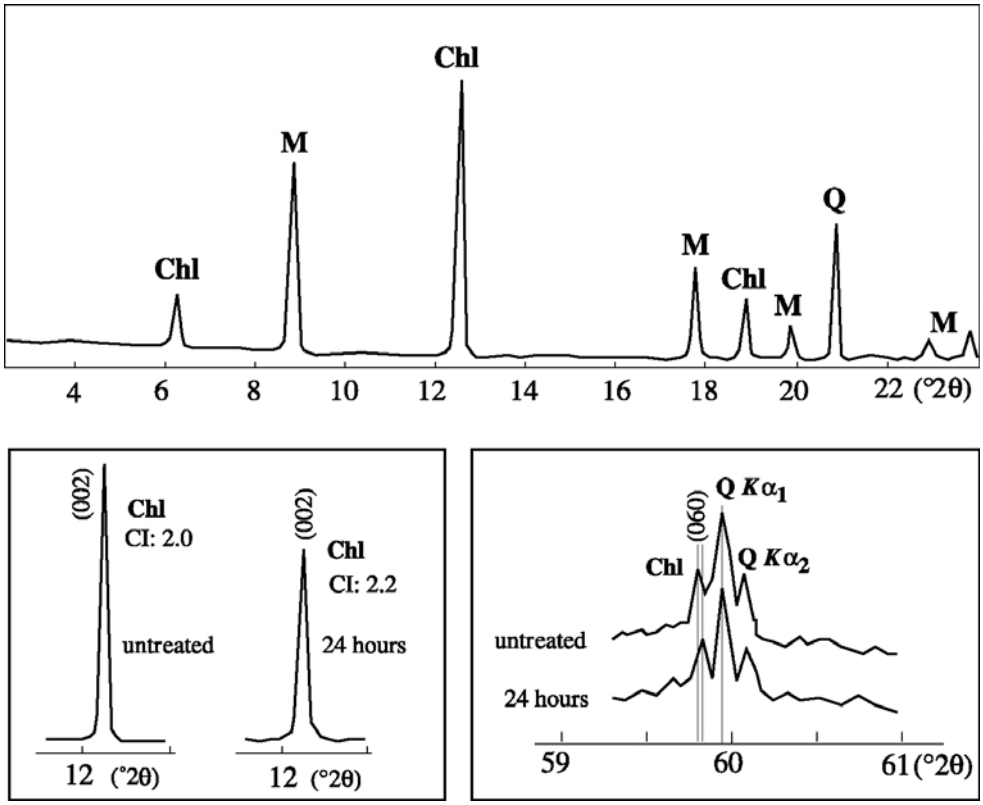

FIG. 2. Smoothed XRD patterns of the Palaeozoic slate sample comparing crystallinity index (CI) and b_o parameter of chlorite before and after acidic river water treatment. Mineral abbreviations: Chl (chlorite), M (mica), Q (quartz); Cu-*K*a radiation.

related to the reduction of the b_o parameter, and consequently the change in proton concentration cannot be a simple result of ionic exchange. Nevertheless, the largest shortening of the b_o parameter occurred after the first 30 min monitoring period, whereas the greatest extent of the Fe loss took place during the 180 min treatment. Therefore, it seems that crystal structure changes happened prior to the chemical decomposition of chlorite, in agrement with previous studies (Ross &

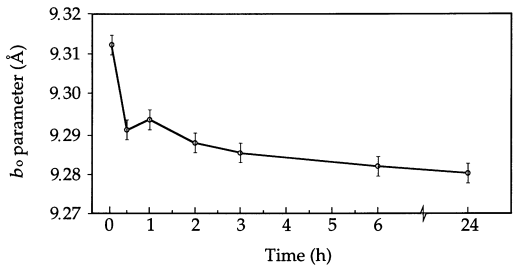

FIG. 3. Variation in the b_o parameter of chlorite from the Palaeozoic slate sample with time, showing the error bars associated with the b_o parameter.

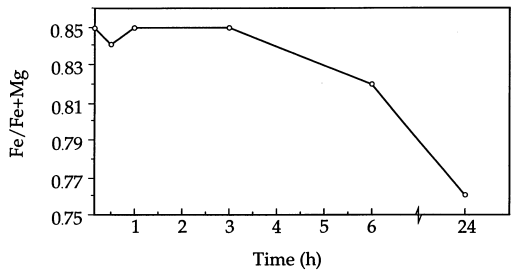

FIG. 4. Variation in the Fe/Fe+Mg ratio of chlorite, as determined by EDS analysis, from the Palaeozoic slate sample with time.

Kodama, 1974; Ross, 1975) which demonstrated conclusively that selective dissolution of chlorite occurs only after the structure has been disturbed, probably as a result of dehydroxylation and oxidation of ferrous iron (Bain, 1972; Makumbi & Herbillon, 1972). In particular, Ross (1975) showed that oxidation of ferrous iron plays a major role in the initiation of the structure disorder required for converting chlorite to vermiculite.

As noted above, monitoring of the oxidation state of Fe in the course of the treatment (Meunier, pers. comm.) is of particular interest. However, controlling the oxidation state of Fe causes serious problems (Velde, 1985), which explains why there is no information on this subject to date. In addition, Fe_2O_3 is a normal component of many chlorites and its presence should not be interpreted as evidence for secondary oxidation (Foster, 1962). It is assumed, therefore, that the octahedral occupancy represents the sum of Mg and total Fe (Fe^{2+}+Fe^{3+}).

On the other hand, the pH values of the aqueous solution shifted from 2.2 to 2.8 in the course of a few minutes, and subsequently remained almost constant due to the low acid-neutralization potential of the rock. In fact, since no neutralizing minerals (e.g. calcite) were present within the slate sample, the water acidity was retained throughout the course of the treatment. This enabled the solubilization of some cations (particularly Fe, Mg and Al) from the solid sample, thus increasing the concentration of these elements in the aqueous solution (Table 2). Iron was by far the most common dissolved element in the solution after short-time treatments. Subsequently some Fe precipitated as oxy-hydroxides because of its very low solubility product (Weast, 1989), even at low pH values, by which the ionic concentration decreased over time. Likewise, there was a decrease in the Ca concentration, which probably resulted from the ionic adsorption onto the active surface of clay minerals rather than precipitation as hydroxide, carbonate or sulphate (under very acid water conditions), according to calculations based on equilibrium constants (Weast, 1989) of the above mentioned species.

Removal of Fe, Mg and Al can be largely attributed to the partial dissolution of chlorite, which is usually considered an unstable phase in acid solutions (Ross, 1969; 1975). The rate of release of the cations was variable during the progress of acid dissolution; thus octahedrally-coordinated Fe was removed more easily than Mg or Al, and so it is regarded as the major mobile component.

Although none of the treated samples showed any common weathering product of chlorite, such as vermiculite or regularly interstratified chlorite-vermiculite (Makumbi & Herbillon, 1972; Ross & Kodama, 1974, 1976; Murakami *et al*., 1996), the Fe and Mg ions released from the octahedral sites of the structure clearly reflect an incipient alteration of chlorite into vermiculitic products. The neoformation of vermiculite from dissolved chlorite is chemically characterized by the loss of ferrous ions from the 2:1 layers together with the release of Mg from the hydroxide sheets, as claimed by Proust (1982) and Proust *et al*. (1986). Our experimental alteration of chlorite into vermiculite was not

TABLE 2. Chemical composition and pH values of the water river sample before and after different lengths of treatment with chlorite-bearing slate.

Samples	pH	Mg		Ca		Na		K		Fe		Al		Si	
		(1)	(2)	(1)	(2)	(1)	(2)	(1)	(2)	(1)	(2)	(1)	(2)	(1)	(2)
River water	2.2	63.0		268		58		14		106		68		2.2	
30 min	2.8	83.0	39	185	−161	51.5	−13	3.7	−20	206	194	88	39	6.6	9
60 min	2.8	82.5	37	187	−153	51	−13	1.4	−24	209	194	90	41	8.0	11
120 min	2.9	82.5	36	192	−142	49	−17	1.6	−23	203	181	88	37	10.8	16
180 min	2.9	83.5	35	194	−129	50.5	−13	1.6	−21	184	135	86	31	8.0	10
360 min	2.9	83.5	37	194	−137	52.5	−10	2.8	−20	152	85	87	35	5.2	6
1 day	2.9	84.0	41	186	−160	51	−14	5.0	−18	132	51	85	33	9.4	14

(1) ppm in aqueous solution
(2) ppm/g extracted from the sample

successful, probably because greater lengths of time are required to complete the reaction. Nevertheless, the occurrence of mixed-layered chlorite-vermiculite in the river bed sediments of the nearby Odiel river (Requena *et al*., 1991) provides natural evidence of the transformation of chlorite into vermiculite.

It is likely that most of the extracted Al comes from the octahedral rather than tetrahedral sites, as shown by Brindley & Youell (1951) after progressive acid attack on chlorite samples, suggesting that the tetrahedral sheet of the chlorite structure was not significantly altered by the acid water. A further observation supporting this assumption is the negligible silica content extracted from the chlorite-bearing slate to the aqueous solution. Therefore, a preferential extraction of octahedral cations can be deduced from our experimental results.

Smectite-rich clay. Contrary to the chlorite-bearing slate, treated and untreated samples of the smectite-rich sediment differ in mineral composition (Table 1). When compared to the starting material, the persistence of illite and kaolinite is notable, as is the disappearance of smectite and calcite soon after treatment (Fig. 5), which is in good agreement with the general lack of these minerals in sediments suspended in the Tinto river (Fernández-Caliani *et al*., 1996; Galán *et al*., 1996).

Despite the extreme hydrogeochemical conditions, illite and kaolinite did not show appreciable variations in crystal chemistry parameters during the experiment because of their high chemical stability (Konta, 1991). In contrast, as a result of the lower resistance of smectite in acidic environments (e.g. Kittrick, 1971; Novak & Cicel, 1978), this expandable phyllosilicate was dramatically dissolved in the river water, as indicated by the disappearance of their characteristic diffraction peaks and the chemical changes detected in the fluid composition within the first 30 min of treatment.

The total decomposition of smectite resulted in removal of octahedral Al, Mg and Fe, as well as tetrahedral Si and Al, thus increasing the concentration of these cations in the aqueous solution. Unfortunately, in this acidic weathering system the physicochemical conditions are not well-fixed, and so the fluid composition cannot be easily interpreted in terms of simple thermodynamic diagrams. Because of the extremely high dissolution rate of smectite, no direct evidence is available for the mechanisms controlling the dissolution process. Luca & MacLachlan (1992) reported that acid treatment appears to remove tetrahedral and octahedral Fe from the smectite structure at about the same rate, and Tkac *et al*. (1994) found little difference in the rate of acid dissolution of octahedral and tetrahedral Al in smectites, although in no case was the rate for octahedral Al greater than that for tetrahedral Al.

Likewise, calcite was dissolved and the pH values of the solution shifted from 2.2 to 6.6, buffering almost neutral conditions in water. The sudden increase of the pH is readily explained by the dissolution of calcite available within the sediment, which rapidly neutralized the water acidity. Obviously, the disappearance of smectite in the short-time treated sample leads to the conclusion that this clay mineral dissolved at a faster rate than calcite, when the river water was still acidic. All neutralizing calcite was consumed and large amounts of Ca were removed during treatment. Thus, the occurrence of authigenic gypsum on the flood plain of the Tinto river (Fernández-Caliani & Galán, 1997) can be explained experimentally by precipitation of the Ca-saturated sulphate waters, as a result of the acid neutralization.

Neutral conditions after calcite breakdown triggered precipitation of Fe and Al oxy-hydroxides and silica gels from the solution, and neoformation of amorphous silicate phases largely enriched in Al and Mg, which explain the lack of Fe, Al and Si, as well as the decrease of Mg concentration in the extracted fluid (Table 3). These poorly crystalline phases and amorphous components of the acid-treated samples, which were identified from SEM-EDS observations, can be regarded as the final reaction products of the smectite dissolution.

Finally, it must be emphasized that these experimental results are in good agreement with field observations, especially for Fe oxy-hydroxides which are prevalent in ochreous overbank sediments of the Tinto river.

CONCLUSIONS

This experiment establishes that natural weathering processes driven by acid mine drainage are responsible for the progressive degradation of chlorites, as seen through the selective alteration of the octahedral sheets and the shortening of the *b* unit-cell parameter, indicating an early stage for the

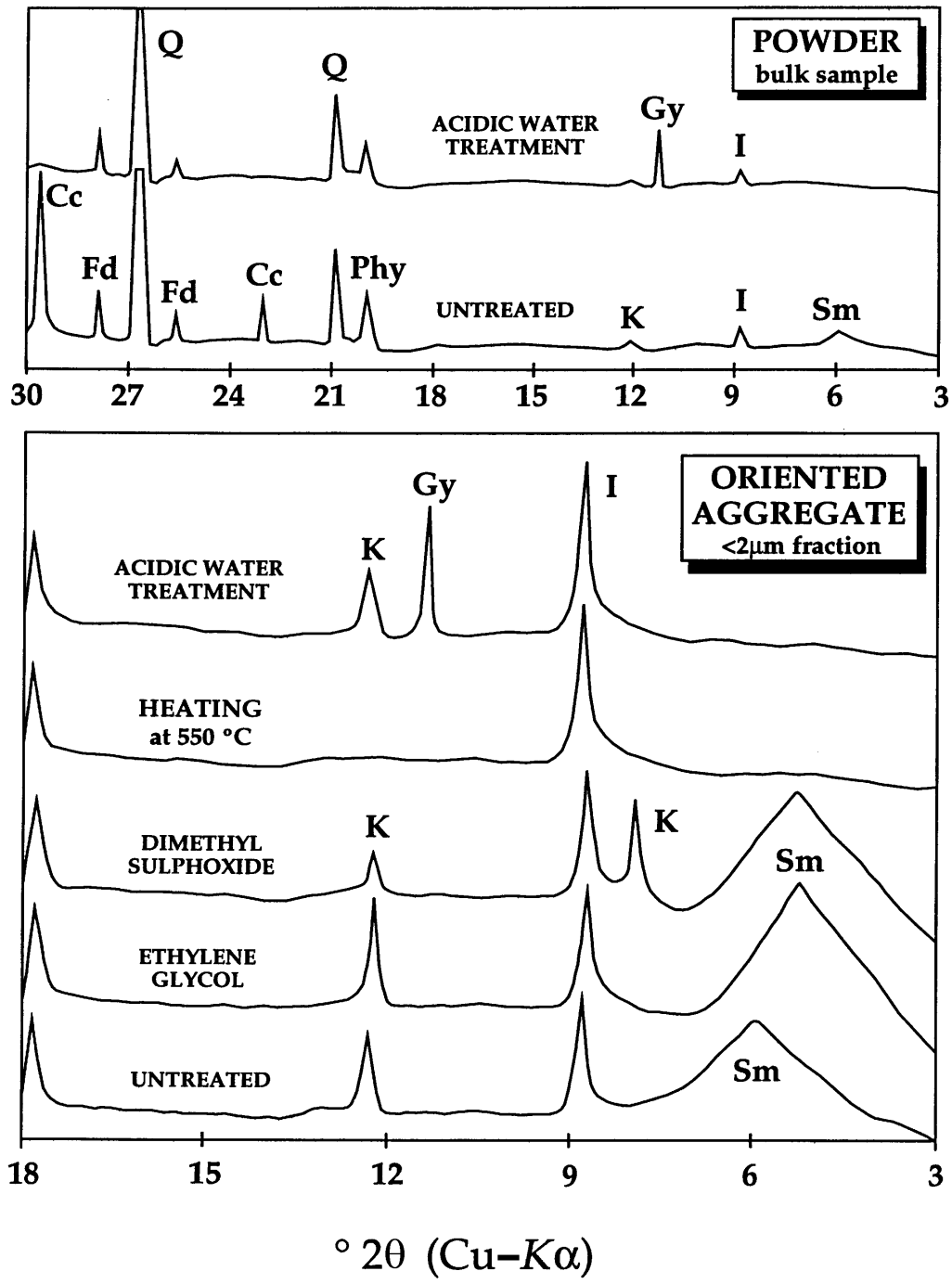

FIG. 5. Smoothed X-ray diffraction patterns of the Miocene smectite-rich sample upon different treatments. Note the disappearance of smectites and formation of gypsum after attack with acidic river water. Mineral abbreviations: Cc (calcite), Fd (feldspar), Gy (gypsum), I (illite), K (kaolinite), Phy (phyllosilicates), Q (quartz), Sm (smectite).

TABLE 3. Chemical composition and pH values of the water river sample before and after different lengths of treatment with smectite-rich marl.

Samples	pH	Mg		Ca		Na		K		Fe		Al		Si	
		(1)	(2)	(1)	(2)	(1)	(2)	(1)	(2)	(1)	(2)	(1)	(2)	(1)	(2)
River water	2.2	63		268		58		14		106		68		2.2	
5 min	6.6	73	18	724	834	56	−4	19	9	0	−106	3	−119	0	−2.2
10 min	6.6	75	23	726	890	58	0	17	6	0	−106	3	−128	0	−2.2
15 min	6.6	74	19	720	784	58	0	19	9	0	−106	2	−114	0	−2.2
30 min	6.6	74	19	686	749	58	0	19	9	0	−106	4	−115	0	−2.2
60 min	6.6	76	25	716	877	55	−6	17	6	0	−106	3	−127	0	−2.2
180 min	6.6	77	25	734	847	52	−11	19	9	0	−106	4	−116	0	−2.2

(1) ppm in aqueous solution
(2) ppm/g extracted from the sample

transformation of chlorite into vermiculitic products. Likewise, the river sediments are devoid of smectite and calcite by the acid water effect, which leads to both dissolution of these phases and co-precipitation on the river banks of inorganic amorphous components largely enriched in Fe, Si and Al. Although the data from this experimental simulation are in good agreement with field observations, further research is still required, to examine in more detail the generalized reactions above.

ACKNOWLEDGMENTS

We would like to thank A. Meunier and two anonymous reviewers for their help in improving the manuscript.

REFERENCES

Bailey S.W. (1972) Determination of chlorite composition by X-ray spacings and intensities. *Clays Clay Miner.* **20**, 381–388.

Bain D.C. (1972) Oxidation of chlorites in soil clays and effect on DTA curves. *Nature Physical Sci.* **238**, 142–143.

Brindley G.W. & Youell R.F. (1951) A chemical determination of tetrahedral and octahedral aluminium ions in a silicate. *Acta Cryst.* **4**, 495–496.

Cabrera F., Conde B. & Flores V. (1992) Heavy metals in the surface sediments of the tidal river Tinto (SW Spain). *Fresenius Envir. Bull.* **1**, 400–405.

Elbaz-Poulichet F. & Leblanc M. (1996) Transfer de métaux d'une province minière á l'océan par des fleuves acides (Río Tinto, Espagne). *C.R. Acad. Sci. Paris,* **322**, 1047–1052.

Fernández-Caliani J.C. & Galán E. (1997) Formación de yeso autigénico en la llanura de inundación del río Tinto (Huelva). Implicaciones paleoambientales. *Geogaceta,* **21**, 103–106.

Fernández-Caliani J.C., Requena A. & Galán E. (1996) Clay mineralogy and heavy metal content of suspended sediments in an extremely polluted environment: the Tinto river. Preliminary report. Pp. 218–220 in: *Advances in Clay Minerals* (M. Ortega-Huertas, A. López-Galindo & I. Palomo, editors). Univ. Granada, Spain.

Foster M.D. (1962) Interpretation of the composition and classification of the chlorites. *U.S. Geological Survey Professional Paper,* **414-A**, 33 p.

Galán E. & González I. (1993) Contribución de la mineralogía de arcillas a la interpretación de la evolución paleogeográfica del sector occidental de la Cuenca del Guadalquivir. *Estudios Geol.* **49**, 261–275.

Galán E., Requena A. & Fernández-Caliani J.C. (1996) Provenance and evolution of clay minerals in the Tinto river, SW Spain. *Geol. Carpathica-Clays,* **5**, 61–66.

García-Palomero F. (1980) *Caracteres Geológicos y Relaciones Morfológicas y Genéticas de los Yacimientos del Anticlinal de Riotinto.* Inst. Est. Onubenses, Huelva, 262 pp.

Kisch H.J. (1991) Illite cystallinity: Recommendations on sample preparation, X-ray diffraction settings and interlaboratory samples. *J. Metam. Geol.* **9**, 665–670.

Kittrick J.A. (1971) Montmorillonite equilibria and the weathering environment. *Soil Sci. Soc. Am. Proc.* **35**, 815–820.

Konta J. (1991) Phyllosilicate in rivers: Result of weathering, erosion, transportation and deposition. Pp. 23–44 in: *Conferencias* (E. Galán & M. Ortega-Huertas, editors). XI Reunión Sociedad Española de

Arcillas.

Luca V. & MacLachlan D.J. (1992) Site occupancy in nontronite studied by acid dissolution and Mössbauer spectroscopy. *Clays Clay Miner.* **40**, 1–7.

Makumbi L. & Herbillon A.J. (1972) Vermiculitization éxperimentale d'une chlorite. *Bull. Groupe Franç. Argiles*, **24**, 153–165.

Martín Pozas J.M. (1975) Análisis cuantitativo de fases cristalinas por difracción de rayos X. In: *Método de Debey-Scherrer* (J. Saja, editor). ICE. Univ. Valladolid.

Moore D.M. & Reynolds R.C. (1989) *X-ray Diffraction: Identification and Analysis of Clay Minerals*, pp. 224–225. Oxford Univ. Press.

Murakami T., Isobe H., Sato T. & Ohnuki T. (1996) Weathering of chlorite in a quartz-chlorite schist: I. Mineralogical and chemical changes. *Clays Clay Miner.* **44**, 244–256.

Nelson C.H. & Lamothe P.J. (1993) Heavy metal anomalies in the Tinto and Odiel river and estuary system, Spain. *Estuaries,* **16**, 496–511.

Novak I. & Cicel B. (1978) Dissolution of smectites in hydrochloric acid: II. Dissolution rate as a function of crystallochemical composition. *Clays Clay Miner.* **26**, 341–344.

Proust D. (1982) Supergene alteration of metamorphic chlorite in an amphibolite from Massif Central, France. *Clay Miner.* **17**, 159–173.

Proust D., Emery J.P. & Beaufort D. (1986) Supergene vermiculitization of a magnesian chlorite: Iron and magnesium removal processes. *Clays Clay Miner.* **34**, 572–580.

Requena A., Clauss F.L. & Fernández-Caliani J.C. (1991) Mineralogía y aspectos geoquímicos de los sedimentos actuales del río Odiel (Huelva). *Cuad. Xeol. Laxe,* **16**, 135–144.

Ross G.J. (1969) Acid dissolution of chlorites: Release of magnesium, iron and aluminium and mode of acid attack. *Clays Clay Miner.* **17**, 347–354.

Ross G.J. (1975) Experimental alteration of chlorites into vermiculites by chemical oxidation. *Nature,* **255**, 133–134.

Ross G.J. & Kodama H. (1974) Experimental transformation of a chlorite into a vermiculite. *Clays Clay Miner*. **22**, 205–211.

Ross G.J. & Kodama H. (1976) Experimental alteration of a chlorite into a regularly interstratified chlorite-vermiculite by chemical oxidation. *Clays Clay Miner.* **24**, 183–190.

Schermerhörn L.J.G. (1971) An outline stratigraphy of the Iberian Pyrite Belt. *Bol. Geol. Min.* **82**, 239–268.

Schultz L.G. (1964) Quantitative interpretation of mineralogical composition from X-ray and chemical data for the Pierre Shale. *U.S. Geol. Surv. Prof. Paper*, **391-C**, 39 pp.

Tkac I., Komadel P. & Müller D. (1994) Acid-treated montmorillonites. A study by ^{29}Si and ^{27}Al MAS NMR. *Clay Miner.* **29**, 11–19.

Velde B. (1985) *Clay Minerals: A Physico-Chemical Explanation of their Occurrence*. Elsevier, Amsterdam.

Weast R.C. (1989) *Handbook of Chemistry and Physics.* Pp. B207–B208, D50–D93. CRC Press, Boca Raton, Florida (70th edition).